Article

Identifying Diurnal Variability of Brain Connectivity Patterns Using Graph Theory

Farzad V. Farahani [1,*], Magdalena Fafrowicz [2,3,*], Waldemar Karwowski [1], Bartosz Bohaterewicz [2,4], Anna Maria Sobczak [2], Anna Ceglarek [2], Aleksandra Zyrkowska [2], Monika Ostrogorska [5], Barbara Sikora-Wachowicz [2], Koryna Lewandowska [2], Halszka Oginska [2], Anna Beres [2], Magdalena Hubalewska-Mazgaj [6] and Tadeusz Marek [2]

[1] Computational Neuroergonomics Laboratory, Department of Industrial Engineering and Management Systems, University of Central Florida, Orlando, FL 32816, USA; wkar@ucf.edu
[2] Department of Cognitive Neuroscience and Neuroergonomics, Institute of Applied Psychology, Jagiellonian University, 31-007 Kraków, Poland; bartosz.bohaterewicz@uj.edu.pl (B.B.); ann.marie.sobczak@gmail.com (A.M.S.); anna.ceglarek@uj.edu.pl (A.C.); aleksandra.zyrkowska@uj.edu.pl (A.Z.); barbara.wachowicz@uj.edu.pl (B.S.-W.); koryna.lewandowska@uj.edu.pl (K.L.); halszka.oginska@uj.edu.pl (H.O.); a.beres@uj.edu.pl (A.B.); marek@uj.edu.pl (T.M.)
[3] Malopolska Centre of Biotechnology, Jagiellonian University, 31-007 Kraków, Poland
[4] Department of Psychology of Individual Differences, Psychological Diagnosis, and Psychometrics, Institute of Psychology, University of Social Sciences and Humanities, 03-815 Warsaw, Poland
[5] Chair of Radiology, Medical College, Jagiellonian University, 31-007 Kraków, Poland; monika.cichocka@uj.edu.pl
[6] Department of Drug Addiction Pharmacology, Maj Institute of Pharmacology, Polish Academy of Sciences, 01-224 Kraków, Poland; magdalena.hubalewska@uj.edu.pl
* Correspondence: farzad.vasheghani@knights.ucf.edu (F.V.F.); magda.fafrowicz@uj.edu.pl (M.F.)

check for updates

Abstract: Significant differences exist in human brain functions affected by time of day and by people's diurnal preferences (chronotypes) that are rarely considered in brain studies. In the current study, using network neuroscience and resting-state functional MRI (rs-fMRI) data, we examined the effect of both time of day and the individual's chronotype on whole-brain network organization. In this regard, 62 participants (39 women; mean age: 23.97 ± 3.26 years; half morning- versus half evening-type) were scanned about 1 and 10 h after wake-up time for morning and evening sessions, respectively. We found evidence for a time-of-day effect on connectivity profiles but not for the effect of chronotype. Compared with the morning session, we found relatively higher small-worldness (an index that represents more efficient network organization) in the evening session, which suggests the dominance of sleep inertia over the circadian and homeostatic processes in the first hours after waking. Furthermore, local graph measures were changed, predominantly across the left hemisphere, in areas such as the precentral gyrus, putamen, inferior frontal gyrus (orbital part), inferior temporal gyrus, as well as the bilateral cerebellum. These findings show the variability of the functional neural network architecture during the day and improve our understanding of the role of time of day in resting-state functional networks.

Keywords: brain connectivity; resting-state fMRI; circadian rhythm; chronotypes; graph theory

1. Introduction

Most living organisms express a rhythmic cycle across a 24 h period (circadian rhythm) that controls several physiological processes such as sleep–wake patterns [1,2], metabolic activity [3], and body temperature [4], as well as various brain functions [5] such as attention [6], working memory [7], decision bias [8], motor [9], and visual detection [10] tasks.

As well as circadian rhythms, individuals have biologically different inclinations for when to sleep and when they are at their highest alertness and energy level, which are

referred to as chronotypes [11]. Accordingly, people can be divided into morning-type (or early larks), evening-type (or night owls), and intermediate-type (or "neither-type") [12]; the circadian typology moves toward later hours in night owls compared with early larks [13]. Chronotype differences have been reported to be highly influential to people's cognition, behavior, and daily neural activity [1,5,12,14–16].

Although effects of circadian rhythms and chronotypes on whole-brain connectivity have been examined (some cases have only considered time of day [17]), the results are often contradictory and inconsistent. For example, a group of researchers believe that resting-state brain networks maintain a constant topological organization throughout the day [18,19], while others believe that brain networks, especially default mode, sensorimotor, and visual networks, show significant changes as the day progresses when we are at rest [20–22]. Additionally, Orban et al. [23], contrary to the common belief that "global brain signal is low in the morning and then increases in the midafternoon, and drops in the early evening", showed that the global signal fluctuation is continuously decreasing during the day.

Utilizing a combination of graph-based knowledge and noninvasive imaging modality such as functional MRI (fMRI) helps to investigate (locally or globally) the brain functional connectivity at high temporal resolution [24–29]. In recent years, several studies have been conducted to identify topological changes in the brain networks that help us better understand the mechanisms underlying human cognition and neurological disorders [30–39]. For example, Lunsford-Avery et al. (2020) studied the relation between the regularity of sleep/wake patterns and brain connectome among adolescents and young adults to measure how these naturalistic patterns contribute to default mode network (DMN) topology [31]. In another study, Farahani et al. (2019) examined the effects of sleep restriction on the brain functional network and found significant topological alterations mostly across the limbic system, DMN, and visual network [33]. Disrupted brain network topology was examined in studies on patients with Parkinson's disease [32], chronic insomnia [36], major depressive disorder [39], as well as preterm infants [35].

The main purpose of this study is to examine variations of neural activity at different times of the day in both chronotypes and detect circadian fluctuations of brain functional networks using rs-fMRI data. Based on our previous findings, we hypothesized that topological changes were mostly because of time of day rather than chronotype, and areas such as the default mode and sensorimotor networks underwent the most changes. To this end, we apply a graph-theoretic framework to extract the global and local changes in functional connectivity patterns and determine the informative regions that differ during the course of the day. Furthermore, we examine whether graph properties are correlated with the cognitive variables derived from the assessments and questionnaires across participants. The results provide a better understanding of the functional topology of the brain at rest over the course of the day.

2. Materials and Methods

2.1. Participants

Through online announcements, 5354 volunteers were selected to fill out the Chronotype Questionnaire [40] for assessing circadian preferences, the Epworth Sleepiness Scale (ESS) [41] for measuring daytime sleepiness, as well as a sleep–wake assessment. A total of 451 participants divided into morning (MT) or evening types (ET) were selected for PER3 VNTR polymorphism genotyping—only the subjects who were homozygous for the PER3 5/5 alleles (MT) and PER3 4/4 alleles (ET) were included. The procedure resulted in 73 healthy and young individuals in both chronotypes. Other selection criteria included age between 20 and 35 years, right-handedness (assessed by the Edinburgh Handedness Inventory [42]), no sleep deprivation, no neurological illness, and normal or corrected-to-normal vision. The selected individuals were scanned twice, first about 1 h (morning session) and then 10 h (evening session) after waking up. Session order was counter-balanced across participants. The final research sample for further analysis consisted of

62 subjects (39 women, mean age: 23.97 $\pm$ 3.26 years). Participants were asked to have adequate sleep for 1 week before the experiment, and actigraphs were used to monitor their sleep length and quality during that week as well as during the experiment days. Participants were prohibited from consuming alcohol (2 days) and caffeine (1 day) before the scanning sessions, and to refrain from strenuous activity during the experiment. The Ethics Committee for Biomedical Research at the Military Institute of Aviation Medicine, (Warsaw, Poland; 26 February 2013) and the Institute of Applied Psychology Ethics Committee of the Jagiellonian University (Kraków, Poland; 21 February 2017) approved the study, and an informed consent was obtained from all participants in accordance with the Declaration of Helsinki. Demographics, questionnaires, and actigraphy results are provided in Table 1.

Table 1. Demographics, questionnaires, and actigraphy results.

Variables (Mean $\pm$ SD)	MT (n = 31)	ET (n = 31)	Significance
Sex (M/F) [a]	11/20	12/19	$X^2(1) = 0.069$; $p = 0.793$
Age (years) [b]	24.45 $\pm$ 3.83	23.48 $\pm$ 2.55	$U(62) = 446$; $p = 0.623$
ME [b]	15.71 $\pm$ 2.41	28.45 $\pm$ 2.39	$U(62) < 0.001$; $p < 0.001$
AM [b]	21.47 $\pm$ 3.58	22.26 $\pm$ 3.51	$U(62) = 426$; $p = 0.437$
ESS [b]	5.52 $\pm$ 2.48	5.87 $\pm$ 3.01	$U(62) = 441$; $p = 0.576$
EHI [b]	86.83 $\pm$ 12.92	89.19 $\pm$ 13.93	$U(62) = 414$; $p = 0.330$
VNTR of PER3	5/5	4/4	-
Declared waketime (hh:mm) [c]	07:07 $\pm$ 62 min	07:25 $\pm$ 48 min	$t(60) = -1.90$; $p = 0.062$
Declared bedtime (hh:mm) [c]	23:24 $\pm$ 55 min	00:06 $\pm$ 49 min	$t(60) = -3.50$; $p = 0.001$
Declared length of perfect sleep (hh:mm) [c]	08:50 $\pm$ 42 min	08:38 $\pm$ 54 min	$t(60) = 1.54$; $p = 0.128$
Actigraphy-derived waketime (hh:mm) [c]	07:43 $\pm$ 70 min	08:16 $\pm$ 69 min	$t(60) = -1.28$; $p = 0.168$
Actigraphy-derived bedtime (hh:mm) [c]	23:58 $\pm$ 58 min	00:48 $\pm$ 58 min	$t(60) = -3.13$; $p = 0.002$
Actigraphy-derived length of real sleep (hh:mm) [c]	07:53 $\pm$ 51 min	07:36 $\pm$ 40 min	$t(60) = -1.18$; $p = 0.266$

MT—morning types, ET—evening types, ME—morningness/eveningness scale (Chronotype Questionnaire), AM—amplitude scale (Chronotype Questionnaire), ESS—Epworth Sleepiness Scale, EHI—Epworth Handedness Inventory, [a] chi-square test, [b] Mann–Whitney U test, [c] Student's *t*-test.

2.2. Data Acquisition

Magnetic resonance imaging scans were performed using a 3T Siemens Skyra MRI system with a 64-channel head coil. Structural images were collected for each participant using a sagittal three-dimensional T1-weighted MPRAGE sequence. Functional resting-state blood oxygenation level-dependent (BOLD) signals were obtained through a gradient-echo single-short echo planar imaging sequence (10 min/run) using the following parameters: repetition time/echo time (TR/TE) = 1800/27 ms; field of view = 256 $\times$ 256 mm^2; slice thickness = 4 mm (no gap); voxel size = 4 $\times$ 4 $\times$ 4 mm^3. A total of 34 interleaved transverse slices and 335 volumes were obtained from selected participants. During the resting state, participants were instructed to lie in the scanner with their eyes open while thinking of nothing, and to remain awake throughout the scanning session. Participants' awakeness was monitored by an eye tracking system (Eyelink 1000, SR Research, Mississauga, ON, Canada).

2.3. Data Preprocessing

Data were preprocessed using DPABI v. 4.2 and SPM 12, both working under Matlab v.2018a (The Mathworks Inc., Natick, MA, USA). To avoid instability of the initial MRI signals, the first 10 time points were discarded, and the data were then corrected for slice timing and head motion. Participants with movements in one or more of the orthogonal directions above 3 mm or rotation above 3° were excluded from the analysis; four participants were excluded due to excessive head movements. Subsequently, functional scans were coregistered using T1 images and normalized to the Montreal Neurological Institute (MNI) space using DARTEL [43] and a voxel size of 3 $\times$ 3 $\times$ 3 mm^3. In total, seven participants were excluded because of the low quality of the normalization. The functional data were spatially smoothed with a 4 mm Full Width at Half Maximum (FWHM) kernel.

The 24 motion parameters that were derived from the realignment step were regressed out from the functional data by linear regression, as well as five principal components from both cerebrospinal fluid and white matter signals using principal components analysis integrated in a component-based noise correction method [44]. The global signal was included because of its potential in providing additional valuable information [45], and the signal was band-pass filtered (0.01–0.1 Hz).

2.4. Network Construction and Analysis

In this study, we parcellated the whole brain into 116 distinct regions of interest (ROIs; 90 cortical and subcortical and 26 cerebellar) using the automated anatomical labeling (AAL) atlas [46]. The average time courses across all voxels within each region were extracted. Next, by means of Pearson's correlation coefficients, we calculated the pairwise functional connectivity between ROIs. The results were transformed using Fisher's r-to-z transformation for better normalization. Thus, a symmetrical adjacency matrix with a size of 116 × 116 was built for each participant (Figure 1). We applied a density-based thresholding on the obtained networks to maintain the strongest links and eliminate weaker ones [47]. The network density was set between 0.05 and 0.275 with a step of 0.025. Finally, we binarized the matrices to overcome the complexity issue.
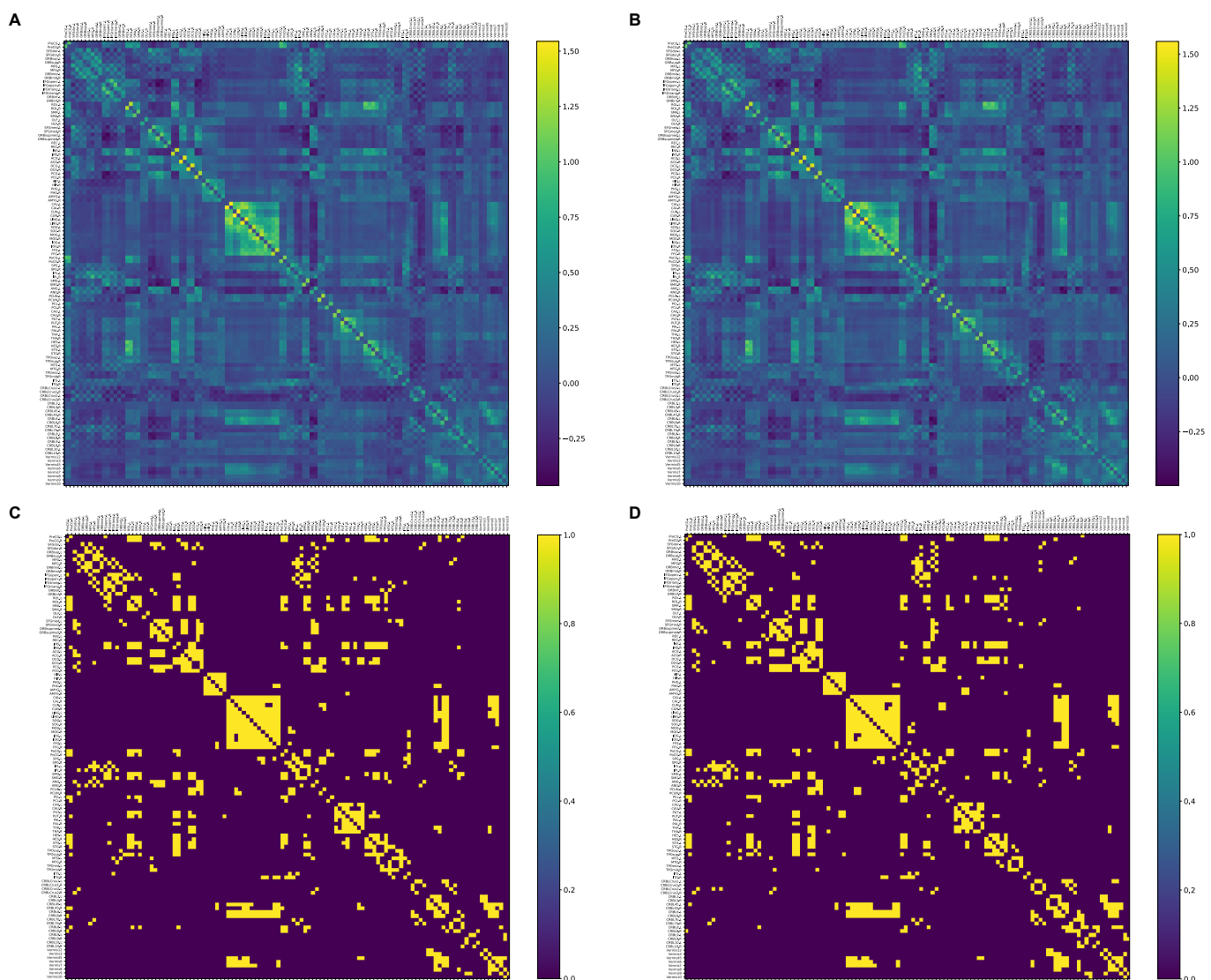

Figure 1. Correlation matrices (**A**,**B**) (transformed Fisher's r-to-z) and 10% binarized matrices (**C**,**D**) for morning and evening sessions, respectively (averaged across all participants in each session). See Appendix A Table A1 for the description of the areas.

2.5. Graph Measure Computation

We extracted a set of global and local properties of the binary networks for each participant using the Brain Connectivity Toolbox (BCT) [28]. Global properties such as global efficiency, modularity, average shortest path, small-worldness, and assortativity can be used to provide global information flow and functional specialization. Local properties such as degree, betweenness centrality, nodal efficiency, nodal clustering coefficient, and participant coefficient (for details on the measures see [28]), were computed for each region separately, reflecting the centrality of nodes and existence of hubs (connector or provincial) in the network. All measures were extracted from the thresholded and binarized networks with the sparsity between 0.05 and 0.275 (step of 0.025). The reason for choosing this interval was to reduce computational complexity while preventing the creation of disconnected graphs.

3. Results

3.1. Global Analysis

We found a significant increase in small-worldness (the ratio of normalized clustering coefficient to normalized path length) from the morning to the evening session (Figure 2) at higher densities ($p < 0.01$, Bonferroni corrected), whereas the changes were not significant in terms of chronotypes. No significant variations were observed for other global measures.
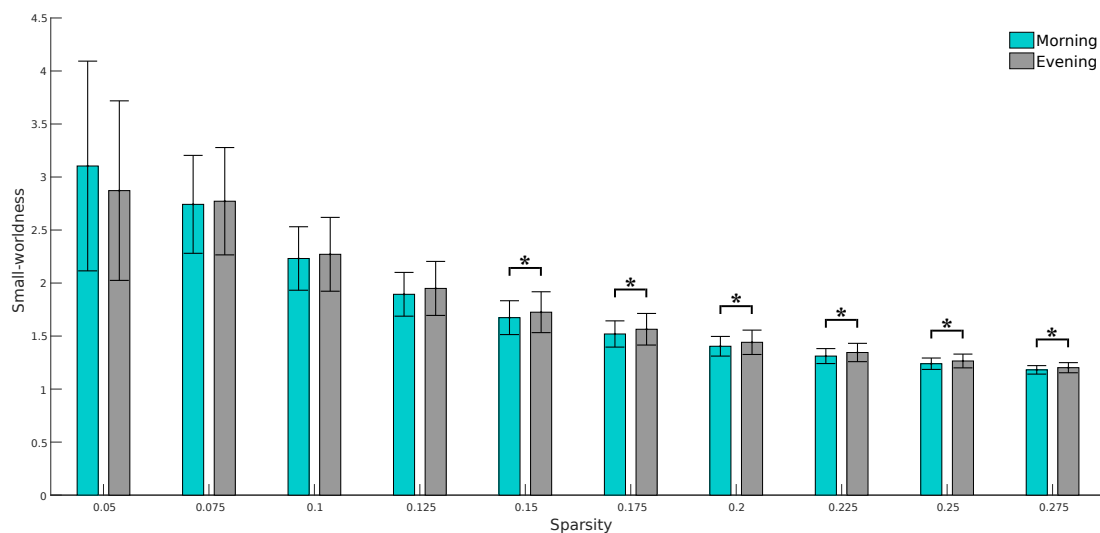

Figure 2. Results of paired *t*-test on the small-worldness at the threshold values of 0.05 to 0.275. Asterisks (*) in the figures show a significant difference in small-worldness between sessions ($p < 0.01$, Bonferroni corrected).

3.2. Local Analysis

Table 2 shows the results of the paired *t*-test on the brain regions that differed statistically between the morning and evening sessions using local metrics, including degree centrality, betweenness centrality, clustering coefficient, and nodal efficiency. According to Table 2, several meaningful changes were evident, mostly across the left hemisphere, in areas such as the precentral gyrus, orbital part of inferior frontal gyrus, lentiform nucleus (particularly the putamen), inferior temporal gyrus, and a series of regions inside the cerebellum. No significant differences were observed for other local measures ($p > 0.001$, Bonferroni corrected). Moreover, the results of degree centrality and betweenness centrality of all 116 brain areas are visualized in Figure 3. Compared with the morning session, the evening session showed significantly decreased degree centrality in the left precentral gyrus, the dorsolateral part of left superior frontal gyrus, the left supplementary motor area, the supramarginal and angular gyri of the left inferior parietal lobe, the left putamen, the left thalamus, and bilateral inferior temporal gyrus, and increased degree centrality in some areas within the cerebellum ($p < 0.001$, Bonferroni corrected).
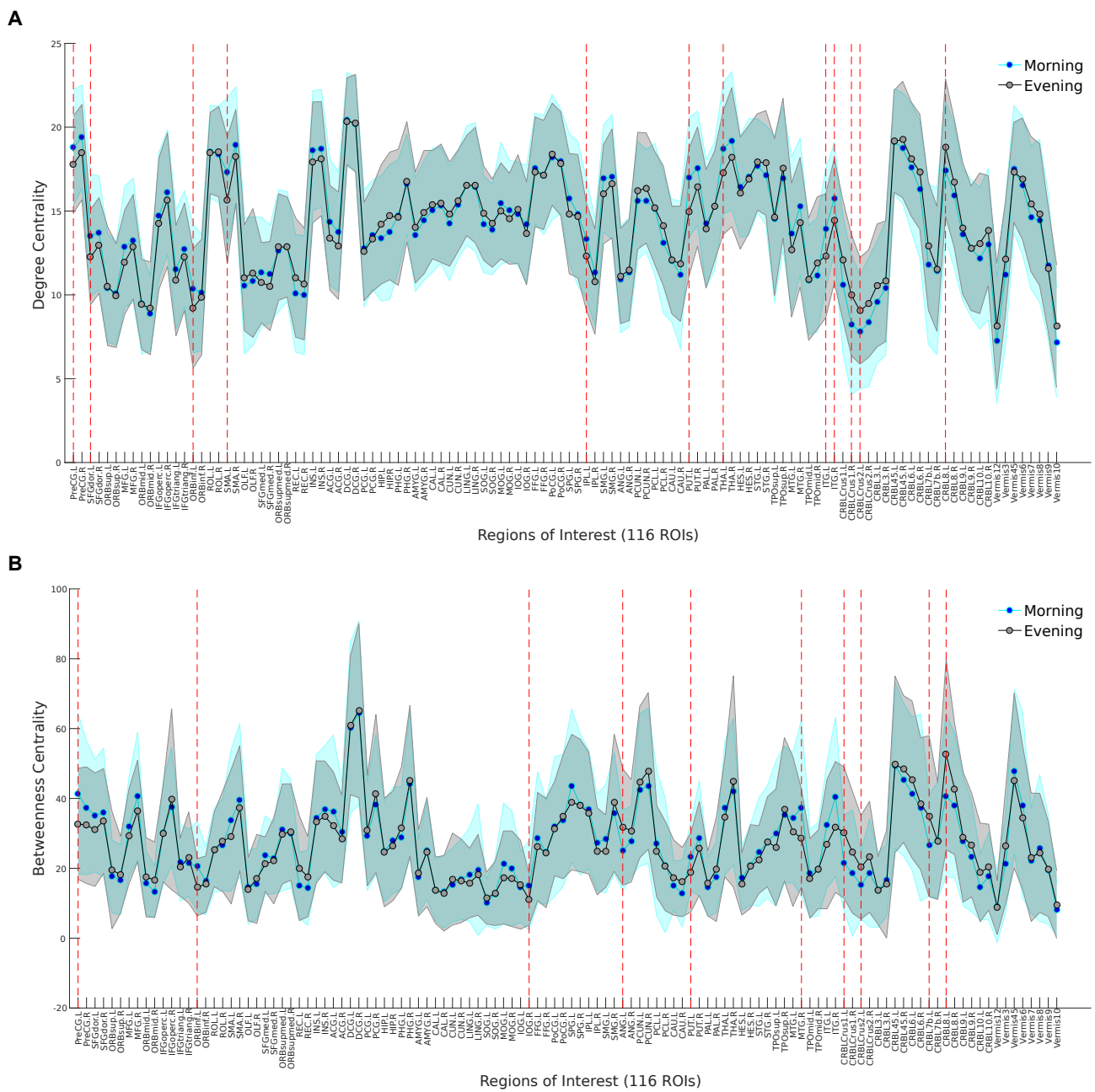
Figure 3. Area under the curve in the morning session (blue) and the evening session (gray) for degree centrality (**A**) and betweenness centrality (**B**) of all 116 brain regions. Significant diurnal fluctuations are represented by red lines. See Table A1 for the description of the areas.

Table 2. List of brain regions of interest (ROIs) that changed throughout the day (significance level was set at $p < 0.01$ and p-values were adjusted for the Bonferroni correction).

ROI (Network)	MNI Coordinates			AAL Label	p-Value			
	x	**y**	**z**		**DC**	**BC**	**CC**	**NE**
1 (DMN)	−38.65	−5.68	50.94	Precentral_L	0.00043	0.00021		0.00024
3 (DMN)	−18.45	34.81	42.20	Frontal_Sup_L	0.00040			0.00045
15 (FPN)	−35.98	30.71	−12.11	Frontal_Inf_Orb_L	0.00043	0.00003		0.00025
19 (SMN)	−5.32	4.85	61.38	Supp_Motor_Area_L	0.00015			0.00010
54 (VN)	38.16	−81.99	−7.61	Occipital_Inf_R		0.00030		
61 (FPN)	−42.80	−45.82	46.74	Parietal_Inf_L	0.00042			0.00042

Table 2. *Cont.*

ROI (Network)	MNI Coordinates			AAL Label	*p*-Value			
	x	y	z		DC	BC	CC	NE
63 (SMN)	−55.79	−33.64	30.45	SupraMarginal_L	0.00065			0.00044
65 (FPN)	−44.14	−60.82	35.59	Angular_L		0.00004		
73 (LS)	−23.91	3.86	2.40	Putamen_L	0.00002	0.00043		0.00002
77 (LS)	−10.85	−17.56	7.98	Thalamus_L	0.00043			0.00046
78 (LS)	13.00	−17.55	8.09	Thalamus_R			0.00014	
83 (FPN)	−39.88	15.14	−20.18	Temporal_Pole_Sup_L			0.00033	
86 (DMN)	57.47	−37.23	−1.47	Temporal_Mid_R		0.00025		
89 (VN)	−49.77	−28.05	−23.17	Temporal_Inf_L	0.00015			0.00011
90 (VN)	53.69	−31.07	−22.32	Temporal_Inf_R	0.00028	0.00060		0.00029
91 (CRB)	−35.00	−67.00	−29.00	Cerebellum_Crus1_L	0.00066	0.00006		0.00069
92 (CRB)	38.00	−67.00	−30.00	Cerebellum_Crus1_R	0.00011	0.00081		0.00008
93 (CRB)	−28.00	−73.00	−38.00	Cerebellum_Crus2_L	0.00033	0.00037		0.00022
94 (CRB)	33.00	−69.00	−40.00	Cerebellum_Crus2_R	0.00096			0.00073
101 (CRB)	−31.00	−60.00	−45.00	Cerebellum_7b_L		0.00035		
103 (CRB)	−25.00	−55.00	−48.00	Cerebellum_8_L	0.00039	0.00006		0.00059
107 (CRB)	−22.00	−34.00	−42.00	Cerebellum_10_L		0.00052		

DC—Degree Centrality, BC—Betweenness Centrality, CC—Clustering Coefficient, NE—Nodal Efficiency.

3.3. Hub Analysis

We also identified network hubs along with their types (i.e., connector or provincial) in morning and evening sessions within the sensorimotor, visual, frontoparietal, default mode, limbic, and cerebellar networks (Table 3). The results are based on the mean connectivity matrix (across all participants for each corresponding session) and a network density of 0.1. According to Table 3, differences between the two sessions were located in regions such as the left supramarginal gyrus; right superior temporal pole; right thalamus; left lobule VIII of cerebellar hemisphere; and lobules IV, V, and VI of vermis. Interestingly, the sensorimotor network was the densest part of the brain at rest with the most hubs (mostly provincial, i.e., within modular connections) compared with the other networks. In contrast, the hubs in default mode, limbic, and cerebellar networks were mainly connector type (i.e., between modular connections).

Table 3. Hub regions in different brain networks (at a sparsity of 0.1).

Network	Morning		Evening	
	L	R	L	R
Sensorimotor	Rolandic_Oper_L [P] Insula_L [P] Postcentral_L [P] SupraMarginal_L [P] Temporal_Sup_L [P]	Rolandic_Oper_R [P] Insula_R [P] Postcentral_R [P] SupraMarginal_R [C] Temporal_Sup_R [P]	Rolandic_Oper_L [P] Insula_L [P] Postcentral_L [P] - Temporal_Sup_L [P]	Rolandic_Oper_R [P] Insula_R [P] Postcentral_R [P] SupraMarginal_R [C] Temporal_Sup_R [P]
Visual	Lingual_L [P] Fusiform_L [P]	Lingual_R [P] Fusiform_R [P]	Lingual_L [P] Fusiform_L [P]	Lingual_R [P] Fusiform_R [P]
Frontoparietal	-	-	-	Temporal_Pole_Sup_R [C]
Default Mode	Precentral_L [C]	Precentral_R [C]	Precentral_L [C]	Precentral_R [C]
Limbic	Cingulum_Mid_L [C] -	Cingulum_Mid_R [C] Thalamus_R [P]	Cingulum_Mid_L [C] -	Cingulum_Mid_R [C] -
Cerebellar	Cerebellum_4_5_L [C] Cerebellum_6_L [C] Vermis_4_5 [P]	Cerebellum_4_5_R [C] Cerebellum_6_R [C] -	Cerebellum_4_5_L [C] Cerebellum_6_L [C] Cerebellum_8_L [C] Vermis_6 [P]	Cerebellum_4_5_R [P] Cerebellum_6_R [C] - -

L/R—Left or Right Hemisphere, P—Provincial, C—Connector.

3.4. Correlation Analysis

Finally, we performed correlation analyses to examine the associations between local measures and questionnaire scores (e.g., morningness/eveningness (ME) scale, amplitude (AM) scale, and ESS). The results are displayed in Table 4 ($p < 0.01$, Bonferroni corrected). For the morning session, we found significant negative associations between ME score and nodal properties of right hippocampus and right parahippocampal gyrus, as well as positive associations between ME score and nodal metrics (degree and nodal efficiency) of the right lenticular nucleus and pallidum. We found significant positive associations between AM score and nodal metrics (degree and nodal efficiency) of the left precentral gyrus and left postcentral gyrus, as well as negative associations between AM score and degree and betweenness centrality of the right lobule X of cerebellum. Finally, the only significant correlation with ESS score was its positive associations with degree and nodal efficiency of the left postcentral gyrus. In the evening session, we found significant negative associations between AM score and nodal metrics (nodal clustering coefficient and local efficiency) of the right hippocampus, as well as positive associations between ME score and degree centrality of the right pallidum. Furthermore, positive and negative correlations were observed for ME and AM, respectively, with nodal metrics within the left parahippocampal gyrus. No significant correlations were found between ESS and brain metrics.

Table 4. Partial correlations between nodal metrics with ME, AM, and ESS scores ($n = 62$; significance level was set at $p < 0.01$ and p-values were adjusted for the Bonferroni correction).

	ROI	Local Metrics	Partial Correlation (p-Value)		
			ME	**AM**	**ESS**
Morning	Hippocampus_R	Degree Centrality	−0.408 (0.0020)	-	-
		Nodal Efficiency	−0.361 (0.0080)	-	-
	ParaHippocampal_R	Nodal Clustering Coefficient	−0.367 (0.0068)	-	-
		Nodal Local Efficiency	−0.374 (0.0054)	-	-
	Pallidum_R	Degree Centrality	0.424 (0.0010)	-	-
		Nodal Efficiency	0.445 (0.0006)	-	-
	Precentral_L	Degree Centrality	-	0.361 (0.0080)	-
		Nodal Efficiency	-	0.402 (0.0024)	-
		Nodal Shortest Path	-	−0.465 (0.0002)	-
	Postcentral_L	Degree Centrality	-	0.395 (0.0030)	0.388 (0.0036)
		Nodal Efficiency	-	0.407 (0.0020)	0.358 (0.0086)
		Nodal Shortest Path	-	−0.410 (0.0018)	-
	Cerebellum_10_R	Degree Centrality	-	−0.378 (0.0048)	-
		Betweenness Centrality	-	−0.377 (0.0050)	-
Evening	Hippocampus_R	Nodal Clustering Coefficient	-	−0.440 (0.0006)	-
		Nodal Local Efficiency	-	−0.467 (0.0002)	-
	ParaHippocampal_L	Nodal Local Efficiency	-	−0.356 (0.0092)	-
		Nodal Shortest Path	0.382 (0.0044)	-	-
	Pallidum_R	Degree Centrality	0.353 (0.0098)	-	-

ME—Morningness/Eveningness Scale, AM—Amplitude Scale, ESS—Epworth Sleepiness Scale.

4. Discussion

In this paper, we investigated the effect of time of day and the individual's chronotype on the functional brain networks of 62 healthy participants using rs-fMRI data and a graph-based approach. In the global analysis, we found that small-worldness increased over the course of the day ($p < 0.01$, Bonferroni corrected). In the local analysis, we identified significant diurnal variations, mostly across the left hemisphere, in areas including the precentral gyrus, putamen, inferior frontal gyrus (orbital part), inferior temporal gyrus, as well as in the bilateral cerebellum ($p < 0.001$, Bonferroni corrected). In the hub analysis, we found that the sensorimotor network was the densest area of the brain (in terms of hub numbers) in both the morning and evening sessions with primarily provincial type

hubs, whereas hubs in default mode, limbic, and cerebellar networks were mostly of the connector type. The effect of chronotype and interaction between time of day and chronotype (so-called synchrony effect) were not observed in global and local analyses, which is in line with our previous study [48]. The synchrony effect was confirmed in a variety of cognitive domains [5,49] and in task fMRI characterized by high complexity [15]. In relation to the resting-state data, some recent reports revealed the influence of chronotype on resting-state functional connectivity (with contradicting results) [50,51]; however, they did not confirm the synchrony effect. Our findings regarding global and local connectivity profiles indicate the variability of the brain's functional organization between morning and evening resting-state sessions as a universal phenomenon, independent of circadian typology. Finally, in the correlation analysis, we found evidence of associations between questionnaire scores and local metrics in several regions in both sessions, mostly related to morning. In the following, we discuss in more detail the significant diurnal changes related to small-worldness, local characteristics, hub, and correlation analysis.

4.1. Diurnal Variations in Small-Worldness

A small-world network is an intermediary between random and regular networks, consisting of a large number of short-range connections together with a few long-range shortcuts [52]. Mathematically, small-world networks have a high clustering coefficient and short average path length, which makes them superior to other networks in terms of functional segregation and integration, respectively [28,53]. A higher small-worldness global property of brain networks has been shown in younger versus older individuals [54] and in healthy controls compared with patients with Alzheimer's disease [55]. According to our rs-fMRI findings, a lower value of small-worldness in the morning compared with the evening reflects a less efficient functional topology and greater wiring cost. The results could be explained by an effect called "sleep inertia", which is believed to be the third process (Process W) of sleep regulation together with circadian rhythm (Process C) and homeostatic process (Process S) [56]. It refers to the transitional state between sleep and wake, characterized by impaired performance and reduced vigilance in the minutes or even hours after waking up [57]. This conflicts with the common intuitive belief that in the morning hours, the brain is recovered after the full night of sleep and should work most effectively. The occurrence and length of sleep inertia depend on the individual and on the sleep stage in which waking occurred or on previous sleep deprivation [58,59]. However, the exact function and neurophysiological basis of sleep inertia are still not fully known (for a review see [56]). Vallat et al. (2019) suggest that this phenomenon is caused by the loss of functional brain network segregation from the default mode network, which is also observed during sleep and periods of elevated sleepiness. Then, a progressive restoration of the functional segregation of the brain networks is possibly responsible for sleep inertia dissipation after awakening [60].

In the present study, we found that the global small-worldness index was higher in the evening after the whole day of functioning, compared with the morning, regardless of the participant's chronotype. Results on small-worldness of human brain networks in relation to time of day and participant fatigue level remain mixed and even contradictory. Our results are in line with observations made by Liu et al. (2014) [61], who found that small-worldness properties of resting-state networks in sleep-deprived individuals are higher than those in well-rested individuals. Researchers have interpreted this effect as an indicator of a compensatory reorganization of the human brain network under conditions of resource shortages. In the current study, participants had good quality and length of sleep the night before the experiment, which was confirmed by data obtained from their wrist actigraphs. However, these results can be interpreted as possibly related to the homeostatic process [62] that is in control of sleep regulation and accumulates during time spent awake.

4.2. Diurnal Variations in Nodal Properties

In this subsection, we discuss the topological changes of the brain regions across the day in detail. Our findings here are classified based on the predefined brain networks in this study, that is, default mode network, frontoparietal network, sensorimotor network, visual network, limbic system, and cerebellar network.

4.2.1. Default Mode Network (DMN)

Our results showed that time of day affected degree, betweenness centrality, and nodal efficiency in the precentral, superior frontal, and middle temporal gyri. These results can be seen as a proof of DMN variability through the day. The DMN was initially presumed to be exceptionally active when the mind is not focused, being in a state of wakeful rest and wandering [63]. The DMN is thought to be implicated in various aspects of self-referential processing [64], such as thinking about ourselves, remembering the past, and making plans for the future [65], and it is sometimes referred to as an anti-task network because the DMN is deactivated during goal-oriented tasks [66,67]. Diurnal variation of DMN was also found in the study of Jiang et al. (2016) [17], which revealed increased regional homogeneity (ReHo) and amplitude of low-frequency fluctuations (ALFF) in the morning hours compared with the evening. Results of this study are congruent with ours, showing that the precentral gyrus, also known as the primary motor cortex, is more significant for the network in the morning hours. However, Jiang et al. (2016) [17] observed decreased ReHo and ALFF in the superior frontal gyrus in the morning resting-state procedure, whereas our results indicated higher nodal efficiency of the same region in the morning. The superior frontal gyrus is thought to be associated with higher cognitive functions; however, its contribution remains obscure [68]. Disagreement in current studies investigating circadian rhythms prompts further exploration of the aforementioned subject. A meta-analysis by Fusar-Poli et al. (2009) [69] found that increased activity of the middle temporal gyrus (MTG) was present when participants were presented with emotional faces. The MTG was also identified as being recruited in automatic semantic processing and being especially active during demanding task execution [70].

A recent study by Xu et al. (2019) shed some light on the functional complexity of the MTG [71]. These authors identified four sub-regions, each with different specialization in, among others, social cognition and semantic and language processing, demonstrating MTG involvement in many cognitive functions. Our results showed increased betweenness centrality in the right MTG during the morning session compared with the evening session. Higher values of betweenness centrality suggest that MTG as a node participates in a large number of shortest paths, being a hub-like node, such that, on average, more information will pass through MTG than other nodes inside a network.

4.2.2. Frontoparietal Network (FPN)

Diurnal changes were also observed in regard to local properties of the FPN, the network involved in executive control [72]. Similar to that in other brain networks, these alterations were observed in the left hemisphere. First, the orbital part of the left inferior frontal gyrus showed decreased degree centrality and betweenness centrality in the evening compared with the morning session. Additionally, the left inferior parietal lobe showed an analogous pattern of diurnal differences, with lower degree centrality in the evening compared with the morning hours. Taken together, these results show that both the inferior frontal and inferior parietal lobes have fewer functional connections with other brain networks in the evening, and the inferior frontal gyrus also had fewer short paths, which may suggest that its role is less central to the network in the evening [28]. Importantly, part of the parietal lobe, the left angular gyrus, showed higher betweenness centrality in the evening than in the morning. This might suggest that whereas the role of inferior frontal gyrus is diminished in the evening, the role of left angular gyrus becomes more central to the network, because a higher fraction of short paths is typical for the bridging nodes [28]. The left inferior gyrus is linked, among others, to inhibitory control

of responses [73], whereas the left inferior parietal cortex is linked to attention shifting and mediating attentional flexibility [74]. Accordingly, increased resting-state functional connectivity between the left angular gyrus and other brain regions has been linked to sustained attention deficits in patients with multiple sclerosis [75]. In addition, diurnal changes in other local property measures, such as nodal efficiency, were present in both the left inferior frontal and parietal regions, whereas the left superior temporal pole showed diurnal variations in clustering coefficient. These findings reveal diurnal variability in local integration within the neighborhood of the inferior frontal and parietal nodes, as well as changes in clustered connectivity, that is, in the interconnectedness of nodes within the neighborhood of the left superior temporal pole [28]. Taken together, our results suggest that the control processes mediated by the FPN are less efficient in the evening hours, especially in terms of inhibition. Consistently, time-of-day effects on the brain activity of the frontal and parietal regions and on related processes have been demonstrated in previous studies [76,77].

4.2.3. Sensorimotor Network (SMN)

The SMN, involved in the processing of sensory information and motor reactions, has diurnal rhythmicity, as confirmed by several studies [20,78]. In the current study, two nodes that are part of the SMN—the supplementary motor area and supramarginal gyrus—had different degree centrality and nodal efficiency according to the time of day. A previous study revealed that the left supplementary motor area has increased functional connectivity in the evening hours [48], which indicates alterations in daily activity of the SMN. The results of the current study are in contrast to previous results, showing fewer connections coming out of this structure in the evening, according to the graph measures. In reference to the supramarginal gyrus, Song et al. (2018) demonstrated the synchrony effect, such that evening types showed higher activity during the evening session compared with morning types [79]. We did not observe this synchrony effect in any of the graph measures; however, the study of Song et al. (2018) [79] was conducted using task fMRI, not resting-state fMRI.

4.2.4. Visual Network (VN)

The within-subject variability in VN is well known [80,81]; for example, sleep debt and self-reported "sleepiness" are positively correlated with functional connectivity in the VN [82,83]. However, VN changes regarding time of day have not been thoroughly examined. In our study, diurnal variability was found in this network, regardless of the participant's chronotype. In the right inferior occipital gyrus (IOG.R), we found different betweenness centrality according to the time of day. In the left inferior temporal gyrus (ITG.L), alterations in degree centrality and nodal efficiency were noted. Diurnal variability in the right inferior temporal gyrus (ITG.R) involved all three factors. This means that particular nodes of visual network have fewer functional links and shortest paths to other nodes in the brain in the evening than in the morning. These results are consistent with previous studies, in which a decrease in resting-state functional connectivity was observed between regions of VN from morning to evening [17,48,83,84]. In contrast, Gratton et al. (2018) found no time-of-day effect on VN [85]. According to Cordani et al. (2018) [86], resting-state BOLD signal in the visual cortex increases significantly between 8:00 and 17:00, and then it decreases significantly at 20:00 and increases (but not significantly) again at 23:00. There is still no satisfying and clear explanation of this phenomenon of sensory processing within the circadian VN [87,88]. Cordani et al. (2018) suggested that the human visual cortex is modulated by daylight changes, with compensatory mechanisms at dawn and dusk [86].

4.2.5. Limbic System (LS)

We found two subcortical areas, traditionally considered parts of the LS, that showed differences in local properties depending on the time of day: the putamen and the thalamus. The putamen (one of the basal nuclei) and the caudate nucleus compose the dorsal striatum. Primarily, the structure is thought to play an important role in movement preparation and

execution and in learning [89]. In the context of circadian variability, changes in activation were shown mainly for the left putamen [90]. It has been reported that the putamen response to rewards is lower in the afternoon or early evening compared with that in the morning hours [91,92]. In line with those reports, our findings (i.e., differences in local connectivity indicators) implied that the left putamen is less functionally connected with other brain areas in the evening. The thalamus is seen as a hub that passes sensory and motor information between the cerebral cortex and subcortical areas while taking part in regulation of the sleep–wake cycle [93]. The paraventricular thalamus (PVT) is known to be especially important in this regulation because it is reciprocally connected to the suprachiasmatic nuclei (SCN) and receives photic and circadian timing information [94]. Additionally, the thalamus shows circadian rhythmicity [83]. Here, we found that compared with morning hours, degree centrality in the left thalamus was decreased in the evening. Interestingly, Muto et al. (2016) indicated that subcortical areas, including basal ganglia and the thalamus, exhibit circadian modulation that follows the melatonin profile [83].

4.2.6. Cerebellar Network (CRB)

Graph analyses revealed diurnal differences in the CRB associated with higher measures of network centrality such as nodal efficiency and degree and betweenness centrality in the evening compared with the morning. These results indicate the high ability of bilateral Crus I and II but also left lobules VIIB, VIII, and X of the cerebellar hemisphere to transmit the information to other regions included in the CRB [95]. Dynamic interaction is related to greater efficiency and thereby better functioning of the whole cerebellum, which, apart from basic motor control such as voluntary limb movements, balance, and maintaining posture [96], is associated with the visual attention process and working memory [97]. Diurnal rhythmicity of resting-state cerebellar activity has not been sufficiently examined yet; however, a task study conducted by Bonzano et al. (2016) showed higher morning activity of the cerebellum during both actual and mental movement tasks [98], which is contradictory to our results, which revealed higher efficiency of the CRB during evening fMRI sessions. Sami et al. (2014) showed an association between memory consolidation and Crus II [99], whereas our results revealed larger centrality measures in the same area. Moreover, Tzvi et al. (2015) reported striatal–cerebellar networks to mediate consolidation in a motor learning task [100]. Because of the lack of knowledge on resting-state fMRI time-of-day differences in the CRB, there is a clear need for further investigation.

4.3. Provincial and Connector Hubs

Hubs, a set of highly interconnected brain areas [101], are a set of integrative nodes and have a key role in functional connectivity networks within the human brain [102]. They are involved in transmitting the information across different areas of the brain by incorporating parallel and distributed networks [103] and have a key role in network organization [104]. In the present study, we tested participants twice a day, in the morning and in the evening, to identify the brain hubs under the resting state conditions within both experimental sessions. The analysis recognized the common—for morning and evening—provincial hubs (i.e., within modular connections) as a bilateral rolandic operculum, insula, postcentral gyrus, superior temporal gyrus, lingual gyrus fusiform gyrus, precentral gyrus, midcingulate area, and cerebellum. We also found the common—for both testing sessions—connector hubs (i.e., between modular connections) to be bilateral precentra gyrus, midcingulate area, and lobule VI of the cerebellar hemisphere. The differences between the two experimental sessions were located in regions such as the left supramarginal gyrus; right superior temporal pole; right thalamus; left lobule VIII of cerebellar hemisphere; and lobules IV, V, and VI of the vermis. The sensorimotor network was the densest part of the brain at rest, with the most hubs (mostly provincial) compared with the other networks. In contrast, the hubs in default mode, limbic, and cerebellar networks were mainly connectors.

4.4. Correlation Analysis

Correlation analysis indicates that more evening-oriented individuals (or late chronotypes) show lower degree centrality and nodal efficiency in the right hippocampus, lower nodal clustering coefficient and local efficiency in the right parahippocampal area, and higher degree centrality and nodal efficiency in right pallidum if examined in the morning, and shorter nodal paths in the left parahippocampal area, higher degree centrality in the right pallidum, and higher global assortativity in the evening. This may be interpreted, in a simplified way, so that later chronotype is associated with lower effectiveness of information transmission in the hippocampus and parahippocampal area during morning hours, while the transmission in the pallidum seems to be enhanced—both in the morning and evening. The morningness–eveningness dimension of chronotype refers to diurnal preferences and awareness of own performance level. In this context, lowered information flow in some structures in morning hours may be seen as a key indicator of eveningness. The pallidum node is more challenging to interpret. However, if one pays attention to the hedonic aspects of pallidum functions, it may be interesting to consider it in the context of individual differences in reward system sensitivity. Some research, applying various methodologies, suggest that evening types may be better "equipped" for processing pleasure and reward, e.g., Hasler et al. (2017) found a greater ventral striatum response to winning in young male evening-oriented individuals [105], while results of the cortical thickness analysis of Rosenberg et al. (2018) revealed greater grey matter volumes for late chronotypes in the left anterior insula [106]. Additionally, Norbury (2020) indicated (in a group of older adults) that self-reported eveningness was associated with increased grey matter volume in brain regions implicated in risk and reward processing (bilateral nucleus accumbens, caudate, putamen, and thalamus) and orbitofrontal cortex [107]. Finally, higher global assortativity linked with eveningness and manifested in evening hours may be seen as indirect proof of the accuracy of the subjective ME scale.

More distinct or "stronger" chronotypes (described by higher scores in the AM scale) tend to show lower global clustering coefficient, network local efficiency, and average path length as well as higher degree centrality and nodal efficiency in left precentral and postcentral areas, shorter nodal paths in left precentral and postcentral regions, and lower degree centrality and betweenness centrality in the right cerebellum in the morning, but lower nodal clustering coefficient and local efficiency in the right hippocampus as well as lower nodal local efficiency in the left parahippocampal area in the evening. These results indicate that strong chronotype is associated with effective information transmission in general sensing areas and less effective information transmission in the cerebellum in morning hours and lowered ability of specialized processing in hippocampal and parahippocampal areas in the evening. Subjective circadian amplitude is a complex construct referring to the range of diurnal variations of arousal, reflected in the strength of morning–evening preferences, flexibility, and stability of the rhythm [40]. Without a doubt, diurnal arousal changes indicate emotional lability and may be associated with emotional responsiveness and general sensitivity. Thus, the enhanced information transmission/flow in general sensing areas (precentral and postcentral) seems to be a logical correlate of large diurnal amplitude.

5. Conclusions

In the present study, we employed chronotype-based paradigms and performed graph-theory based network analysis in resting-state functional MRI to explore the topological differences in whole-brain functional networks between morning and evening sessions. The study results revealed meaningful information about the topological alterations of the brain network during the day. The results showed the effect of time of day on the functional connectivity patterns, but with no significant difference in chronotype categories. The chronotype-based paradigm is considered a highly sensitive tool for controlling circadian and homeostatic parameters [5]. The lack of differences between the topological alterations of the brain network during the day in the group of morning and evening-types suggests a universal character of the described phenomenon.

6. Limitations and Future Work

Several limitations in the current study should be considered for future directions. The first limitation concerns the atlas used in this study. We applied the AAL atlas to define 116 (cortical and subcortical) graph nodes for brain network construction. Although there is no consensus on which atlas is optimal for brain parcellation [108], some neuroscientists believe that the AAL atlas leads to inefficient parcel homogeneity [109]. A recommended atlas for handling this issue in future work is the cortical Schaefer/Yeo atlas [110]. Among the many advantages of the Schaefer/Yeo atlas is that each node is preassigned to a system based on a cross-validated study. Yet another limitation concerns the thresholding of the functional matrices. In fact, while thresholding does control for differences in binary density across subjects, it does not mean that the thresholded networks are representative of a given subject. Finally, comparing to the *t* and *F* tests, nonparametric permutation tests provide a more flexible and intuitive method for analyzing the data from functional neuroimaging studies [111]. Applying permutation tests which allow inferences to be made without prior assumptions should be considered in future studies.

Author Contributions: M.F., K.L., B.S.-W., and T.M. designed laboratory experiment. M.F. supervised data collection. M.F., M.O., K.L., B.S.-W., A.B., and M.H.-M. contributed to data collection. M.F., B.B., A.M.S., A.C., A.Z., and M.H.-M. contributed to data preparation. F.V.F. and W.K. conducted data exploration and modeling. F.V.F. prepared the initial draft of the manuscript. M.F., W.K., B.B., A.M.S., A.C., A.Z., M.O., B.S.-W., K.L., H.O., A.B., and T.M. supervised all aspects of manuscript preparation, revision, editing, and final content. All authors contributed to the intellectual content of the manuscript. All authors have read and agreed to the published version of the manuscript.

Institutional Review Board Statement: The study was conducted according to the guidelines of the Declaration of Helsinki, and approved by the Ethics Committees of Biomedical Research at the Military Institute of Aviation Medicine, Warsaw, Poland of (report number 02/2013; 26 February 2013) and Institute of Applied Psychology at the Jagiellonian University, Krakow, Poland (21 February 2017).

Informed Consent Statement: Informed consent was obtained from all subjects involved in the study.

Data Availability Statement: The experimental fMRI data are available with the correspondence M.F., vonfrovitz@gmail.com; magda.fafrowicz@uj.edu.pl.

Conflicts of Interest: The authors declare no conflict of interest.

Appendix A

Table A1. Summary of each parcellation's abbreviation, description, and MNI coordinates.

Abbreviation	Description	MNI Coordinates
SENSORIMOTOR NETWORK (SMN)		
ROL.L	Left Rolandic operculum	−47.16, −8.48, 13.95
ROL.R	Right Rolandic operculum	52.65, −6.25, 14.63
SMA.R	Right supplementary motor area	8.62, 0.17, 61.85
INS.L	Left insula	−35.13, 6.65, 3.44
INS.R	Right insula	39.02, 6.25, 2.08
PoCG.L	Left postcentral gyrus	−42.46, −22.63, 48.92
PoCG.R	Right postcentral gyrus	41.43, −25.49, 52.55
SPG.L	Left superior parietal lobule	−23.45, −59.56, 58.96
SPG.R	Right superior parietal lobule	26.11, −59.18, 62.06

Table A1. *Cont.*

Abbreviation	Description	MNI Coordinates
SMG.L	Left supramarginal gyrus	−55.79, −33.64, 30.45
SMG.R	Right supramarginal gyrus	57.61, −31.5, 34.48
PCL.L	Left paracentral lobule	−7.63, −25.36, 70.07
PCL.R	Right paracentral lobule	7.48, −31.59, 68.09
HES.L	Left transverse temporal gyrus	−41.99, −18.88, 9.98
HES.R	Right transverse temporal gyrus	45.86, −17.15, 10.41
STG.L	Left superior temporal gyrus	−53.16, −20.68, 7.13
STG.R	Right superior temporal gyrus	58.15, −21.78, 6.8
TPOsup.R	Right superior temporal pole	48.25, 14.75, −16.86
	VISUAL NETWORK (VN)	
CAL.L	Left calcarine sulcus	−7.14, −78.67, 6.44
CAL.R	Right calcarine sulcus	15.99, −73.15, 9.4
CUN.L	Left cuneus	−5.93, −80.13, 27.22
CUN.R	Right cuneus	13.51, −79.36, 28.23
LING.L	Left lingual gyrus	−14.62, −67.56, −4.63
LING.R	Right lingual gyrus	16.29, −66.93, −3.87
SOG.L	Left superior occipital gyrus	−16.54, −84.26, 28.17
SOG.R	Right superior occipital gyrus	24.29, −80.85, 30.59
MOG.L	Left middle occipital gyrus	−32.39, −80.73, 16.11
MOG.R	Right middle occipital gyrus	37.39, −79.7, 19.42
IOG.L	Left inferior occipital cortex	−36.36, −78.29, −7.84
IOG.R	Right inferior occipital cortex	38.16, −81.99, −7.61
FFG.L	Left fusiform gyrus	−31.16, −40.3, −20.23
FFG.R	Right fusiform gyrus	33.97, −39.1, −20.18
	FRONTOPARIETAL NETWORK (FPN)	
MFG.L	Left middle frontal gyrus	−33.43, 32.73, 35.46
MFG.R	Right middle frontal gyrus	37.59, 33.06, 34.04
ORBmid.L	Left middle frontal gyrus, orbital part	−30.65, 50.43, −9.62
ORBmid.R	Right middle frontal gyrus, orbital part	33.18, 52.59, −10.73
IFGoperc.L	Left inferior frontal gyrus, pars opercularis	−48.43, 12.73, 19.02
IFGoperc.R	Right inferior frontal gyrus, pars opercularis	50.2, 14.98, 21.41
IFGtriang.L	Left inferior frontal gyrus, pars triangularis	−45.58, 29.91, 13.99
IFGtriang.R	Right inferior frontal gyrus, pars triangularis	50.33, 30.16, 14.17
ORBinf.L	Left inferior frontal gyrus, pars orbitalis	−35.98, 30.71, −12.11
ORBinf.R	Right inferior frontal gyrus, pars orbitalis	41.22, 32.23, −11.91
SMA.L	Left supplementary motor area	−5.32, 4.85, 61.38
IPL.L	Left inferior parietal lobule	−42.8, −45.82, 46.74
IPL.R	Right inferior parietal lobule	46.46, −46.29, 49.54
ANG.L	Left angular gyrus	−44.14, −60.82, 35.59
ANG.R	Right angular gyrus	45.51, −59.98, 38.63
TPOsup.L	Left superior temporal pole	−39.88, 15.14, −20.18
ITG.L	Left inferior temporal gyrus	−49.77, −28.05, −23.17
	DEFAULT MODE NETWORK (DMN)	
PreCG.L	Left precentral gyrus	−38.65, −5.68, 50.94
PreCG.R	Right precentral gyrus	41.37, −8.21, 52.09
SFGdor.L	Left superior frontal gyrus	−18.45, 34.81, 42.2
SFGdor.R	Right superior frontal gyrus	21.9, 31.12, 43.82
ORBsup.L	Left superior frontal gyrus, orbital part	−16.56, 47.32, −13.31
ORBsup.R	Right superior frontal gyrus, orbital part	18.49, 48.1, −14.02
OLF.R	Right olfactory cortex	10.43, 15.91, −11.26
SFGmed.L	Left medial frontal gyrus	−4.8, 49.17, 30.89
SFGmed.R	Right medial frontal gyrus	9.1, 50.84, 30.22
ORBsupmed.L	Left medial orbitofrontal cortex	−5.17, 54.06, −7.4
ORBsupmed.R	Right medial orbitofrontal cortex	8.16, 51.67, −7.13
REC.L	Left gyrus rectus	−5.08, 37.07, −18.14
REC.R	Right gyrus rectus	8.35, 35.64, −18.04
ACG.L	Left anterior cingulate gyrus	−4.04, 35.4, 13.95
ACG.R	Right anterior cingulate gyrus	8.46, 37.01, 15.84

Table A1. *Cont.*

Abbreviation	Description	MNI Coordinates
PCG.L	Left posterior cingulate gyrus	−4.85, −42.92, 24.67
PCG.R	Right posterior cingulate gyrus	7.44, −41.81, 21.87
PCUN.L	Left precuneus	−7.24, −56.07, 48.01
PCUN.R	Right precuneus	9.98, −56.05, 43.77
MTG.L	Left middle temporal gyrus	−55.52, −33.8, −2.2
MTG.R	Right middle temporal gyrus	57.47, −37.23, −1.47
ITG.R	Right inferior temporal gyrus	53.69, −31.07, −22.32
	LIMBIC SYSTEM (LS)	
OLF.L	Left olfactory cortex	−8.06, 15.05, −11.46
DCG.L	Left midcingulate area	−5.48, −14.92, 41.57
DCG.R	Right midcingulate area	8.02, −8.83, 39.79
HIP.L	Left hippocampus	−25.03, −20.74, −10.13
HIP.R	Right hippocampus	29.23, −19.78, −10.33
PHG.L	Left parahippocampal gyrus	−21.17, −15.95, −20.7
PHG.R	Right parahippocampal gyrus	25.38, −15.15, −20.47
AMYG.L	Left amygdala	−23.27, −0.67, −17.14
AMYG.R	Right amygdala	27.32, 0.64, −17.5
CAU.L	Left caudate nucleus	−11.46, 11, 9.24
CAU.R	Right caudate nucleus	14.84, 12.07, 9.42
PUT.L	Left putamen	−23.91, 3.86, 2.4
PUT.R	Right putamen	27.78, 4.91, 2.46
PAL.L	Left globus pallidus	−17.75, −0.03, 0.21
PAL.R	Right globus pallidus	21.2, 0.18, 0.23
THA.L	Left thalamus	−10.85, −17.56, 7.98
THA.R	Right thalamus	13, −17.55, 8.09
TPOmid.L	Left middle temporal pole	−36.32, 14.59, −34.08
TPOmid.R	Right middle temporal pole	44.22, 14.55, −32.23
	CEREBELLAR NETWORK (CRB)	
CRBLCrus1.L	Left crus I of cerebellar hemisphere	−36.07, −66.72, −28.93
CRBLCrus1.R	Right crus I of cerebellar hemisphere	37.46, −67.14, −29.55
CRBLCrus2.L	Left crus II of cerebellar hemisphere	−28.64, −73.26, −38.20
CRBLCrus2.R	Right crus II of cerebellar hemisphere	32.06, −69.02, −39.95
CRBL3.L	Left lobule III of cerebellar hemisphere	−8.80, −37.22, −18.58
CRBL3.R	Right lobule III of cerebellar hemisphere	12.32, −34.47, −19.39
CRBL45.L	Left lobule IV, V of cerebellar hemisphere	−15.00, −43.49, −16.93
CRBL45.R	Right lobule IV, V of cerebellar hemisphere	17.20, −42.86, −18.15
CRBL6.L	Left lobule VI of cerebellar hemisphere	−23.24, −59.10, −22.13
CRBL6.R	Right lobule VI of cerebellar hemisphere	24.69, −58.32, −23.65
CRBL7b.L	Left lobule VIIB of cerebellar hemisphere	−32.36, −59.82, −45.45
CRBL7b.R	Right lobule VIIB of cerebellar hemisphere	33.14, −63.18, −48.46
CRBL8.L	Left lobule VIII of cerebellar hemisphere	−25.75, −54.52, −47.68
CRBL8.R	Right lobule VIII of cerebellar hemisphere	25.06, −56.34, −49.47
CRBL9.L	Left lobule IX of cerebellar hemisphere	−10.95, −48.95, −45.90
CRBL9.R	Right lobule IX of cerebellar hemisphere	9.46, −49.50, −46.33
CRBL10.L	Left lobule X of cerebellar hemisphere	−22.61, −33.80, −41.76
CRBL10.R	Right lobule X of cerebellar hemisphere	25.99, −33.84, −41.35
Vermis12	Lobule I, II of vermis	0.76, −38.79, −20.05
Vermis3	Lobule III of vermis	1.38, −39.93, −11.40
Vermis45	Lobule IV, V of vermis	1.22, −52.36, −6.11
Vermis6	Lobule VI of vermis	1.14, −67.06, −15.12
Vermis7	Lobule VII of vermis	1.15, −71.93, −25.14
Vermis8	Lobule VIII of vermis	1.15, −64.43, −34.08
Vermis9	Lobule IX of vermis	0.86, −54.87, −34.90
Vermis10	Lobule X of vermis	0.36, −45.80, −31.68

References

1. Schmidt, C.; Peigneux, P.; Leclercq, Y.; Sterpenich, V.; Vandewalle, G.; Phillips, C.; Berthomier, P.; Berthomier, C.; Tinguely, G.; Gais, S.; et al. Circadian preference modulates the neural substrate of conflict processing across the day. *PLoS ONE* **2012**, *7*, e29658. [CrossRef]
2. Dijk, D.-J.; Lockley, S.W. Invited Review: Integration of human sleep-wake regulation and circadian rhythmicity. *J. Appl. Physiol.* **2002**, *92*, 852–862. [CrossRef]
3. Hastings, M.; O'Neill, J.S.; Maywood, E.S. Circadian clocks: Regulators of endocrine and metabolic rhythms. *J. Endocrinol.* **2007**, *195*, 187–198. [CrossRef]
4. Refinetti, R.; Menaker, M. The circadian rhythm of body temperature. *Physiol. Behav.* **1992**, *51*, 613–637. [CrossRef]
5. Schmidt, C.; Collette, F.; Cajochen, C.; Peigneux, P. A time to think: Circadian rhythms in human cognition. *Cogn. Neuropsychol.* **2007**, *24*, 755–789. [CrossRef]
6. Valdez, P.; Ramírez, C.; García, A.; Talamantes, J.; Armijo, P.; Borrani, J. Circadian rhythms in components of attention. *Biol. Rhythm Res.* **2005**, *36*, 57–65. [CrossRef]
7. Ramírez, C.; Talamantes, J.; García, A.; Morales, M.; Valdez, P.; Menna-Barreto, L. Circadian rhythms in phonological and visuospatial storage components of working memory. *Biol. Rhythm Res.* **2006**, *37*, 433–441. [CrossRef]
8. Lewandowska, K.; Wachowicz, B.; Marek, T.; Oginska, H.; Fafrowicz, M. Would you say "yes" in the evening? Time-of-day effect on response bias in four types of working memory recognition tasks. *Chronobiol. Int.* **2018**, *35*, 80–89. [CrossRef]
9. Edwards, B.; Waterhouse, J.; Reilly, T. The Effects of Circadian Rhythmicity and Time-Awake on a Simple Motor Task. *Chronobiol. Int.* **2007**, *24*, 1109–1124. [CrossRef]
10. Tassi, P.; Pellerin, N.; Moessinger, M.; Eschenlauer, R.; Muzet, A. Variation of visual detection over the 24-h period in humans. *Chronobiol. Int.* **2000**, *17*, 795–805. [CrossRef]
11. Roenneberg, T.; Wirz-Justice, A.; Merrow, M. Life between Clocks: Daily Temporal Patterns of Human Chronotypes. *J. Biol. Rhythms* **2003**, *18*, 80–90. [CrossRef]
12. Adan, A.; Archer, S.N.; Hidalgo, M.P.; Di Milia, L.; Natale, V.; Randler, C. Circadian Typology: A Comprehensive Review. *Chronobiol. Int.* **2012**, *29*, 1153–1175. [CrossRef]
13. Bailey, S.L.; Heitkemper, M.M. Circadian rhythmicity of cortisol and body temperature: Morningness-eveningness effects. *Chronobiol. Int.* **2001**, *18*, 249–261. [CrossRef]
14. Schmidt, C.; Collette, F.; Leclercq, Y.; Sterpenich, V.; Vandewalle, G.; Berthomier, P.; Berthomier, C.; Phillips, C.; Tinguely, G.; Darsaud, A.; et al. Homeostatic sleep pressure and responses to sustained attention in the suprachiasmatic area. *Science* **2009**, *324*, 516–519. [CrossRef]
15. Schmidt, C.; Collette, F.; Reichert, C.F.; Maire, M.; Vandewalle, G.; Peigneux, P.; Cajochen, C. Pushing the Limits: Chronotype and Time of Day Modulate Working Memory-Dependent Cerebral Activity. *Front. Neurol.* **2015**, *6*, 199. [CrossRef]
16. Valdez, P.; Ramírez, C.; García, A. Circadian rhythms in cognitive performance: Implications for neuropsychological assessment. *ChronoPhysiol. Ther.* **2012**, *2*, 81–92. [CrossRef]
17. Jiang, C.; Yi, L.; Su, S.; Shi, C.; Long, X.; Xie, G.; Zhang, L. Diurnal Variations in Neural Activity of Healthy Human Brain Decoded with Resting-State Blood Oxygen Level Dependent fMRI. *Front. Hum. Neurosci.* **2016**, *10*, 634. [CrossRef]
18. Byrne, J.E.M.; Murray, G. The sleep and circadian modulation of neural reward pathways: A protocol for a pair of systematic reviews. *Syst. Rev.* **2017**, *6*, 237. [CrossRef]
19. Biswal, B.B.; Mennes, M.; Zuo, X.N.; Gohel, S.; Kelly, C.; Smith, S.M.; Beckmann, C.F.; Adelstein, J.S.; Buckner, R.L.; Col-combe, S.; et al. Toward discovery science of human brain function. *Proc. Natl. Acad. Sci. USA* **2010**, *107*, 4734–4739. [CrossRef]
20. Blautzik, J.; Vetter, C.; Peres, I.; Gutyrchik, E.; Keeser, D.; Berman, A.; Kirsch, V.; Mueller, S.; Pöppel, E.; Reiser, M.; et al. Classifying fMRI-derived resting-state connectivity patterns according to their daily rhythmicity. *Neuroimage* **2013**, *71*, 298–306. [CrossRef]
21. Hodkinson, D.J.; O'Daly, O.; Zunszain, P.A.; Pariante, C.M.; Lazurenko, V.; Zelaya, F.O.; Howard, M.A.; Williams, S.C.R. Circadian and Homeostatic Modulation of Functional Connectivity and Regional Cerebral Blood Flow in Humans under Normal Entrained Conditions. *J. Cereb. Blood Flow Metab.* **2014**, *34*, 1493–1499. [CrossRef] [PubMed]
22. Park, B.; Kim, J.I.; Lee, D.; Jeong, S.-O.; Lee, J.D.; Park, H.-J. Are brain networks stable during a 24-h period? *Neuroimage* **2012**, *59*, 456–466. [CrossRef] [PubMed]
23. Orban, C.; Kong, R.; Li, J.; Chee, M.W.L.; Yeo, B.T.T. Time of day is associated with paradoxical reductions in global signal fluctuation and functional connectivity. *PLOS Biol.* **2020**, *18*, e3000602. [CrossRef] [PubMed]
24. Bullmore, E.; Sporns, O. Complex brain networks: Graph theoretical analysis of structural and functional systems. *Nat. Rev. Neurosci.* **2009**, *10*, 186–198. [CrossRef]
25. Bullmore, E.; Sporns, O. The economy of brain network organization. *Nat. Rev. Neurosci.* **2012**, *13*, 336–349. [CrossRef]
26. Farahani, F.V.; Karwowski, W.; Lighthall, N.R. Application of Graph Theory for Identifying Connectivity Patterns in Human Brain Networks: A Systematic Review. *Front. Neurosci.* **2019**, *13*, 585. [CrossRef]
27. He, Y.; Evans, A. Graph theoretical modeling of brain connectivity. *Curr. Opin. Neurol.* **2010**, *23*, 341–350. [CrossRef]
28. Rubinov, M.; Sporns, O. Complex network measures of brain connectivity: Uses and interpretations. *Neuroimage* **2010**, *52*, 1059–1069. [CrossRef]
29. Van den Heuvel, M.P.; Sporns, O. Network hubs in the human brain. *Trends Cogn. Sci.* **2013**, *17*, 683–696. [CrossRef]

30. Wang, C.; Song, S.; d'Oleire Uquillas, F.; Zilverstand, A.; Song, H.; Chen, H.; Zou, Z. Altered brain network organization in romantic love as measured with resting-state fMRI and graph theory. *Brain Imaging Behav.* **2020**, *14*, 2771–2784. [CrossRef]

31. Lunsford-Avery, J.R.; Damme, K.S.F.; Engelhard, M.M.; Kollins, S.H.; Mittal, V.A. Sleep/Wake Regularity Associated with Default Mode Network Structure among Healthy Adolescents and Young Adults. *Sci. Rep.* **2020**, *10*, 509. [CrossRef] [PubMed]

32. Díez-cirarda, M.; Strafella, A.P.; Kim, J.; Peña, J.; Ojeda, N. Dynamic functional connectivity in Parkinson's disease patients with mild cognitive impairment and normal cognition. *NeuroImage Clin.* **2018**, *17*, 847–855. [CrossRef] [PubMed]

33. Farahani, F.V.; Fafrowicz, M.; Karwowski, W.; Douglas, P.K.; Domagalik, A.; Beldzik, E.; Oginska, H.; Marek, T. Effects of Chronic Sleep Restriction on the Brain Functional Network, as Revealed by Graph Theory. *Front. Neurosci.* **2019**, *13*, 1087. [CrossRef] [PubMed]

34. Finotelli, P.; Dipasquale, O.; Costantini, I.; Pini, A.; Baglio, F.; Baselli, G.; Dulio, P.; Cercignani, M. Exploring resting-state functional connectivity invariants across the lifespan in healthy people by means of a recently proposed graph theoretical model. *PLoS ONE* **2018**, *13*, e0206567. [CrossRef] [PubMed]

35. Gozdas, E.; Parikh, N.A.; Merhar, S.L.; Tkach, J.A.; He, L.; Holland, S.K. Altered functional network connectivity in preterm infants: Antecedents of cognitive and motor impairments? *Brain Struct. Funct.* **2018**, *223*, 3665–3680. [CrossRef] [PubMed]

36. Li, Z.; Chen, R.; Guan, M.; Wang, E.; Qian, T.; Zhao, C. Disrupted brain network topology in chronic insomnia disorder: A resting-state fMRI study. *NeuroImage Clin.* **2018**, *18*, 178–185. [CrossRef]

37. Markett, S.; Reuter, M.; Heeren, B.; Lachmann, B.; Weber, B.; Montag, C. Working memory capacity and the functional connectome-insights from resting-state fMRI and voxelwise centrality mapping. *Brain Imaging Behav.* **2018**, *12*, 238–246. [CrossRef]

38. Sun, Y.; Lim, J.; Dai, Z.; Wong, K.F.; Taya, F.; Chen, Y.; Li, J.; Thakor, N.; Bezerianos, A. The effects of a mid-task break on the brain connectome in healthy participants: A resting-state functional MRI study. *Neuroimage* **2017**, *152*, 19–30. [CrossRef]

39. Zhi, D.; Calhoun, V.D.; Lv, L.; Ma, X.; Ke, Q.; Fu, Z. Aberrant Dynamic Functional Network Connectivity and Graph Properties in Major Depressive Disorder. *Front. Psychiatry* **2018**, *9*, 339. [CrossRef]

40. Oginska, H.; Mojsa-Kaja, J.; Mairesse, O. Chronotype description: In search of a solid subjective amplitude scale. *Chronobiol. Int.* **2017**, *34*, 1388–1400. [CrossRef]

41. Johns, M.W. A new method for measuring daytime sleepiness: The Epworth sleepiness scale. *Sleep* **1991**, *14*, 540–545. [CrossRef] [PubMed]

42. Oldfield, R.C. The assessment and analysis of handedness: The Edinburgh inventory. *Neuropsychologia* **1971**, *9*, 97–113. [CrossRef]

43. Ashburner, J. A fast diffeomorphic image registration algorithm. *Neuroimage* **2007**, *38*, 95–113. [CrossRef] [PubMed]

44. Behzadi, Y.; Restom, K.; Liau, J.; Liu, T.T. A component based noise correction method (CompCor) for BOLD and perfusion based fMRI. *Neuroimage* **2007**, *37*, 90–101. [CrossRef]

45. Liu, T.T.; Nalci, A.; Falahpour, M. The global signal in fMRI: Nuisance or Information? *Neuroimage* **2017**, *150*, 213–229. [CrossRef]

46. Tzourio-Mazoyer, N.; Landeau, B.; Papathanassiou, D.; Crivello, F.; Etard, O.; Delcroix, N.; Mazoyer, B.; Joliot, M. Automated anatomical labeling of activations in SPM using a macroscopic anatomical parcellation of the MNI MRI single-subject brain. *Neuroimage* **2002**, *15*, 273–289. [CrossRef]

47. Van den Heuvel, M.P.; de Lange, S.C.; Zalesky, A.; Seguin, C.; Yeo, B.T.T.; Schmidt, R. Proportional thresholding in resting-state fMRI functional connectivity networks and consequences for patient-control connectome studies: Issues and recommendations. *Neuroimage* **2017**, *152*, 437–449. [CrossRef]

48. Fafrowicz, M.; Bohaterewicz, B.; Ceglarek, A.; Cichocka, M.; Lewandowska, K.; Sikora-Wachowicz, B.; Oginska, H.; Beres, A.; Olszewska, J.; Marek, T. Beyond the Low Frequency Fluctuations: Morning and Evening Differences in Human Brain. *Front. Hum. Neurosci.* **2019**, *13*, 1–6. [CrossRef]

49. Fabbri, M.; Mencarelli, C.; Adan, A.; Natale, V. Time-of-day and circadian typology on memory retrieval. *Biol. Rhythm Res.* **2013**, *44*, 125–142. [CrossRef]

50. Facer-Childs, E.R.; Campos, B.M.; Middleton, B.; Skene, D.J.; Bagshaw, A.P. Circadian phenotype impacts the brain's resting-state functional connectivity, attentional performance, and sleepiness. *Sleep* **2019**, *42*, zsz033. [CrossRef]

51. Tian, Y.; Chen, X.; Xu, D.; Yu, J.; Lei, X. Connectivity within the default mode network mediates the association between chronotype and sleep quality. *J. Sleep Res.* **2020**, *29*, e12948. [CrossRef] [PubMed]

52. Watts, D.J.; Strogatz, S.H. Collective dynamics of 'small-world' networks. *Nature* **1998**, *393*, 440–442. [CrossRef] [PubMed]

53. Bassett, D.S.; Bullmore, E. Small-world brain networks. *Neuroscientist* **2006**, *12*, 512–523. [CrossRef]

54. Onoda, K.; Yamaguchi, S. Small-worldness and modularity of the resting-state functional brain network decrease with aging. *Neurosci. Lett.* **2013**, *556*, 104–108. [CrossRef] [PubMed]

55. Tait, L.; Stothart, G.; Coulthard, E.; Brown, J.T.; Kazanina, N.; Goodfellow, M. Network substrates of cognitive impairment in Alzheimer's Disease. *Clin. Neurophysiol.* **2019**, *130*, 1581–1595. [CrossRef]

56. Hilditch, C.J.; McHill, A.W. Sleep inertia: Current insights. *Nat. Sci. Sleep* **2019**, *11*, 155–165. [CrossRef]

57. Tassi, P.; Muzet, A. Sleep inertia. *Sleep Med. Rev.* **2000**, *4*, 341–353. [CrossRef]

58. Trotti, L.M. Waking up is the hardest thing I do all day: Sleep inertia and sleep drunkenness. *Sleep Med. Rev.* **2017**, *35*, 76–84. [CrossRef]

59. Dinges, D.F.; Orne, M.T.; Orne, E.C. Assessing performance upon abrupt awakening from naps during quasi-continuous operations. *Behav. Res. Methods Instrum. Comput.* **1985**, *17*, 37–45. [CrossRef]

60. Vallat, R.; Meunier, D.; Nicolas, A.; Ruby, P. Hard to wake up? The cerebral correlates of sleep inertia assessed using combined behavioral, EEG and fMRI measures. *Neuroimage* **2019**, *184*, 266–278. [CrossRef]
61. Liu, Y.; Yu, C.; Zhang, X.; Liu, J.; Duan, Y.; Alexander-Bloch, A.F.; Liu, B.; Jiang, T.; Bullmore, E. Impaired long distance functional connectivity and weighted network architecture in Alzheimer's disease. *Cereb. Cortex* **2014**, *24*, 1422–1435. [CrossRef] [PubMed]
62. Borbély, A.A.; Daan, S.; Wirz-Justice, A.; Deboer, T. The two-process model of sleep regulation: A reappraisal. *J. Sleep Res.* **2016**, *25*, 131–143. [CrossRef]
63. Uddin, L.Q.; Clare Kelly, A.M.; Biswal, B.B.; Xavier Castellanos, F.; Milham, M.P. Functional connectivity of default mode network components: Correlation, anticorrelation, and causality. *Hum. Brain Mapp.* **2009**, *30*, 625–637. [CrossRef] [PubMed]
64. Gusnard, D.A.; Raichle, M.E. Searching for a baseline: Functional imaging and the resting human brain. *Nat. Rev. Neurosci.* **2001**, *2*, 685–694. [CrossRef] [PubMed]
65. Meyer, M.L.; Lieberman, M.D. Social working memory training improves perspective-taking accuracy. *Soc. Psychol. Personal. Sci.* **2016**, *7*, 381–389. [CrossRef]
66. Simpson, J.R.; Drevets, W.C.; Snyder, A.Z.; Gusnard, D.A.; Raichle, M.E. Emotion-induced changes in human medial prefrontal cortex: II. During anticipatory anxiety. *Proc. Natl. Acad. Sci. USA* **2001**, *98*, 688–693. [CrossRef] [PubMed]
67. Raichle, M.E.; MacLeod, A.M.; Snyder, A.Z.; Powers, W.J.; Gusnard, D.A.; Shulman, G.L. A default mode of brain function. *Proc. Natl. Acad. Sci. USA* **2001**, *98*, 676–682. [CrossRef]
68. Boisgueheneuc, F.D.; Levy, R.; Volle, E.; Seassau, M.; Duffau, H.; Kinkingnehun, S.; Samson, Y.; Zhang, S.; Dubois, B. Functions of the left superior frontal gyrus in humans: A lesion study. *Brain* **2006**, *129*, 3315–3328. [CrossRef]
69. Fusar-Poli, P.; Placentino, A.; Carletti, F.; Landi, P.; Allen, P.; Surguladze, S.; Benedetti, F.; Abbamonte, M.; Gasparotti, R.; Barale, F. Functional atlas of emotional faces processing: A voxel-based meta-analysis of 105 functional magnetic resonance imaging studies. *J. Psychiatry Neurosci.* **2009**, *34*, 418–432.
70. Davey, J.; Thompson, H.E.; Hallam, G.; Karapanagiotidis, T.; Murphy, C.; De Caso, I.; Krieger-Redwood, K.; Bernhardt, B.C.; Smallwood, J.; Jefferies, E. Exploring the role of the posterior middle temporal gyrus in semantic cognition: Integration of anterior temporal lobe with executive processes. *Neuroimage* **2016**, *137*, 165–177. [CrossRef]
71. Xu, J.; Lyu, H.; Li, T.; Xu, Z.; Fu, X.; Jia, F.; Wang, J.; Hu, Q. Delineating functional segregations of the human middle temporal gyrus with resting-state functional connectivity and coactivation patterns. *Hum. Brain Mapp.* **2019**, *40*, 5159–5171. [CrossRef] [PubMed]
72. Niendam, T.A.; Laird, A.R.; Ray, K.L.; Dean, Y.M.; Glahn, D.C.; Carter, C.S. Meta-analytic evidence for a superordinate cognitive control network subserving diverse executive functions. *Cogn. Affect. Behav. Neurosci.* **2012**, *12*, 241–268. [CrossRef] [PubMed]
73. Swick, D.; Ashley, V.; Turken, A.U. Left inferior frontal gyrus is critical for response inhibition. *BMC Neurosci.* **2008**, *9*, 102. [CrossRef] [PubMed]
74. Dodds, C.M.; Morein-Zamir, S.; Robbins, T.W. Dissociating Inhibition, Attention, and Response Control in the Frontoparietal Network Using Functional Magnetic Resonance Imaging. *Cereb. Cortex* **2011**, *21*, 1155–1165. [CrossRef]
75. Loitfelder, M.; Filippi, M.; Rocca, M.; Valsasina, P.; Ropele, S.; Jehna, M.; Fuchs, S.; Schmidt, R.; Neuper, C.; Fazekas, F.; et al. Abnormalities of Resting State Functional Connectivity Are Related to Sustained Attention Deficits in MS. *PLoS ONE* **2012**, *7*, e42862. [CrossRef]
76. Marek, T.; Fafrowicz, M.; Golonka, K.; Mojsa-Kaja, J.; Oginska, H.; Tucholska, K.; Urbanik, A.; Beldzik, E.; Domagalik, A. Diurnal patterns of activity of the orienting and executive attention neuronal networks in subjects performing a Stroop-like task: A functional magnetic resonance imaging study. *Chronobiol. Int.* **2010**, *27*, 945–958. [CrossRef]
77. Anderson, J.A.E.; Campbell, K.L.; Amer, T.; Grady, C.L.; Hasher, L. Timing is everything: Age differences in the cognitive control network are modulated by time of day. *Psychol. Aging* **2014**, *29*, 648–657. [CrossRef]
78. Tüshaus, L.; Balsters, J.H.; Schläpfer, A.; Brandeis, D.; O'Gorman Tuura, R.; Achermann, P. Resisting Sleep Pressure: Impact on Resting State Functional Network Connectivity. *Brain Topogr.* **2017**, *30*, 757–773. [CrossRef]
79. Song, J.; Feng, P.; Zhao, X.; Xu, W.; Xiao, L.; Zhou, J.; Zheng, Y. Chronotype regulates the neural basis of response inhibition during the daytime. *Chronobiol. Int.* **2018**, *35*, 208–218. [CrossRef]
80. Laumann, T.O.; Gordon, E.M.; Adeyemo, B.; Snyder, A.Z.; Joo, S.J.; Chen, M.-Y.; Gilmore, A.W.; McDermott, K.B.; Nelson, S.M.; Dosenbach, N.U.F.; et al. Functional System and Areal Organization of a Highly Sampled Individual Human Brain. *Neuron* **2015**, *87*, 657–670. [CrossRef]
81. Bijsterbosch, J.; Harrison, S.; Duff, E.; Alfaro-Almagro, F.; Woolrich, M.; Smith, S. Investigations into within- and between-subject resting-state amplitude variations. *Neuroimage* **2017**, *159*, 57–69. [CrossRef] [PubMed]
82. Stoffers, D.; Diaz, B.A.; Chen, G.; den Braber, A.; van't Ent, D.; Boomsma, D.I.; Mansvelder, H.D.; de Geus, E.; Van Someren, E.J.W.; Linkenkaer-Hansen, K. Resting-State fMRI Functional Connectivity Is Associated with Sleepiness, Imagery, and Discontinuity of Mind. *PLoS ONE* **2015**, *10*, e0142014. [CrossRef] [PubMed]
83. Muto, V.; Jaspar, M.; Meyer, C.; Kussé, C.; Chellappa, S.L.; Degueldre, C.; Balteau, E.; Shaffii-Le Bourdiec, A.; Luxen, A.; Middleton, B.; et al. Local modulation of human brain responses by circadian rhythmicity and sleep debt. *Science* **2016**, *353*, 687–690. [CrossRef] [PubMed]
84. Steel, A.; Thomas, C.; Trefler, A.; Chen, G.; Baker, C.I. Finding the baby in the bath water—Evidence for task-specific changes in resting state functional connectivity evoked by training. *Neuroimage* **2019**, *188*, 524–538. [CrossRef] [PubMed]

85. Gratton, C.; Laumann, T.O.; Nielsen, A.N.; Greene, D.J.; Gordon, E.M.; Gilmore, A.W.; Nelson, S.M.; Coalson, R.S.; Snyder, A.Z.; Schlaggar, B.L.; et al. Functional Brain Networks Are Dominated by Stable Group and Individual Factors, Not Cognitive or Daily Variation. *Neuron* **2018**, *98*, 439–452.e5. [CrossRef]

86. Cordani, L.; Tagliazucchi, E.; Vetter, C.; Hassemer, C.; Roenneberg, T.; Stehle, J.H.; Kell, C.A. Endogenous modulation of human visual cortex activity improves perception at twilight. *Nat. Commun.* **2018**, *9*, 1274. [CrossRef]

87. Brown, S.B.R.E.; Tona, K.-D.; van Noorden, M.S.; Giltay, E.J.; van der Wee, N.J.A.; Nieuwenhuis, S. Noradrenergic and cholinergic effects on speed and sensitivity measures of phasic alerting. *Behav. Neurosci.* **2015**, *129*, 42–49. [CrossRef]

88. Bianciardi, M.; Toschi, N.; Eichner, C.; Polimeni, J.R.; Setsompop, K.; Brown, E.N.; Hämäläinen, M.S.; Rosen, B.R.; Wald, L.L. In vivo functional connectome of human brainstem nuclei of the ascending arousal, autonomic, and motor systems by high spatial resolution 7-Tesla fMRI. *Magn. Reson. Mater. Phys. Biol. Med.* **2016**, *29*, 451–462. [CrossRef]

89. Brovelli, A.; Nazarian, B.; Meunier, M.; Boussaoud, D. Differential roles of caudate nucleus and putamen during instrumental learning. *Neuroimage* **2011**, *57*, 1580–1590. [CrossRef]

90. Byrne, J.E.M.; Tremain, H.; Leitan, N.D.; Keating, C.; Johnson, S.L.; Murray, G. Circadian modulation of human reward function: Is there an evidentiary signal in existing neuroimaging studies? *Neurosci. Biobehav. Rev.* **2019**, *99*, 251–274. [CrossRef]

91. Byrne, J.E.M.; Hughes, M.E.; Rossell, S.L.; Johnson, S.L.; Murray, G. Time of Day Differences in Neural Reward Functioning in Healthy Young Men. *J. Neurosci.* **2017**, *37*, 8895–8900. [CrossRef] [PubMed]

92. Masterson, T.D.; Kirwan, C.B.; Davidson, L.E.; LeCheminant, J.D. Neural reactivity to visual food stimuli is reduced in some areas of the brain during evening hours compared to morning hours: An fMRI study in women. *Brain Imaging Behav.* **2016**, *10*, 68–78. [CrossRef] [PubMed]

93. Jan, J.E.; Reiter, R.J.; Wasdell, M.B.; Bax, M. The role of the thalamus in sleep, pineal melatonin production, and circadian rhythm sleep disorders. *J. Pineal Res.* **2009**, *46*, 1–7. [CrossRef] [PubMed]

94. Colavito, V.; Tesoriero, C.; Wirtu, A.T.; Grassi-Zucconi, G.; Bentivoglio, M. Limbic thalamus and state-dependent behavior: The paraventricular nucleus of the thalamic midline as a node in circadian timing and sleep/wake-regulatory networks. *Neurosci. Biobehav. Rev.* **2015**, *54*, 3–17. [CrossRef]

95. Ma, X.; Jiang, G.; Fu, S.; Fang, J.; Wu, Y.; Liu, M.; Xu, G.; Wang, T. Enhanced Network Efficiency of Functional Brain Networks in Primary Insomnia Patients. *Front. Psychiatry* **2018**, *9*, 46. [CrossRef]

96. Ito, M. *The Cerebellum and Neural Control*; Raven Press: New York, NY, USA, 1984; ISBN 0890041067.

97. Brissenden, J.A.; Somers, D.C. Cortico–cerebellar networks for visual attention and working memory. *Curr. Opin. Psychol.* **2019**, *29*, 239–247. [CrossRef]

98. Bonzano, L.; Roccatagliata, L.; Ruggeri, P.; Papaxanthis, C.; Bove, M. Frontoparietal cortex and cerebellum contribution to the update of actual and mental motor performance during the day. *Sci. Rep.* **2016**, *6*, 30126. [CrossRef]

99. Sami, S.; Robertson, E.M.; Miall, R.C. The Time Course of Task-Specific Memory Consolidation Effects in Resting State Networks. *J. Neurosci.* **2014**, *34*, 3982–3992. [CrossRef]

100. Tzvi, E.; Stoldt, A.; Witt, K.; Krämer, U.M. Striatal–cerebellar networks mediate consolidation in a motor sequence learning task: An fMRI study using dynamic causal modelling. *Neuroimage* **2015**, *122*, 52–64. [CrossRef]

101. Power, J.D.; Schlaggar, B.L.; Lessov-Schlaggar, C.N.; Petersen, S.E. Evidence for Hubs in Human Functional Brain Networks. *Neuron* **2013**, *79*, 798–813. [CrossRef]

102. Sato, J.R.; Biazoli, C.E.; Salum, G.A.; Gadelha, A.; Crossley, N.; Vieira, G.; Zugman, A.; Picon, F.A.; Pan, P.M.; Hoexter, M.Q.; et al. Connectome hubs at resting state in children and adolescents: Reproducibility and psychopathological correlation. *Dev. Cogn. Neurosci.* **2016**, *20*, 2–11. [CrossRef] [PubMed]

103. Hwang, K.; Hallquist, M.N.; Luna, B. The Development of Hub Architecture in the Human Functional Brain Network. *Cereb. Cortex* **2013**, *23*, 2380–2393. [CrossRef] [PubMed]

104. Medaglia, J.D. Graph theoretic analysis of resting state functional MR imaging. *Neuroimaging Clin.* **2017**, *27*, 593–607. [CrossRef] [PubMed]

105. Hasler, B.P.; Casement, M.D.; Sitnick, S.L.; Shaw, D.S.; Forbes, E.E. Eveningness among late adolescent males predicts neural reactivity to reward and alcohol dependence 2 years later. *Behav. Brain Res.* **2017**, *327*, 112–120. [CrossRef] [PubMed]

106. Rosenberg, J.; Jacobs, H.I.L.; Maximov, I.I.; Reske, M.; Shah, N.J. Chronotype differences in cortical thickness: Grey matter reflects when you go to bed. *Brain Struct. Funct.* **2018**, *223*, 3411–3421. [CrossRef] [PubMed]

107. Norbury, R. Diurnal Preference and Grey Matter Volume in a Large Population of Older Adults: Data from the UK Biobank. *J. Circadian Rhythms* **2020**, *18*, 3. [CrossRef] [PubMed]

108. Hayasaka, S.; Laurienti, P.J. Comparison of characteristics between region-and voxel-based network analyses in resting-state fMRI data. *Neuroimage* **2010**, *50*, 499–508. [CrossRef]

109. Gordon, E.M.; Laumann, T.O.; Adeyemo, B.; Huckins, J.F.; Kelley, W.M.; Petersen, S.E. Generation and Evaluation of a Cortical Area Parcellation from Resting-State Correlations. *Cereb. Cortex* **2016**, *26*, 288–303. [CrossRef]

110. Schaefer, A.; Kong, R.; Gordon, E.M.; Laumann, T.O.; Zuo, X.-N.; Holmes, A.J.; Eickhoff, S.B.; Yeo, B.T.T. Local-Global Parcellation of the Human Cerebral Cortex from Intrinsic Functional Connectivity MRI. *Cereb. Cortex* **2018**, *28*, 3095–3114. [CrossRef]

111. Nichols, T.E.; Holmes, A.P. Nonparametric permutation tests for functional neuroimaging: A primer with examples. *Hum. Brain Mapp.* **2002**, *15*, 1–25. [CrossRef]